Heavy Metals Removal from Wastewater by Using Different Kinds of Magnetite Nano-Adsorbents: Effects of Different Organic and Inorganic Coatings on The Removal of Copper and Lead Ions

Saeed Tizro[1], Hadi Baseri[2,*]
[1,2] School of Chemistry, Damghan University, Damghan, I.R. Iran

ARTICLE INFO

Article history:

Received 24 May 2016
Accepted 11 October 2016
Available online 25 December 2016

Keywords:

Nanoadsorbents
Adsorption
Heavy metal ions
Wastewater
Removal efficiency

ABSTRACT

Co-precipitation procedure was applied in order to obtain different kinds of magnetic nanoadsobents for the removal of Pb(II) and Cu(II) toxic metal ions from wastewater samples. The prepared nano-adsorbents were characterized by Fourier transform infrared spectroscopy (FTIR), X-ray diffraction analysis (XRD), scanning electron microscopy (SEM), and thermogravimetric analysis (TGA). The average sizes of these nanoparticles were found to be about 15 to 35 nm. Adsorption studies of heavy metal ions were carried out by batch experiments. Also, pH, temperature, contact time and adsorbent dose were studied as the factors affecting the adsorption of heavy metal ions on the surface of magnetic nano-adsorbents. The optimized values for pH, temperature, contact time and adsorbent dose were 10, 313 K, 50 min and 0.2 g, respectively. Also, the maximum amount of removal efficiency for pb^{2+} and Cu^{2+} ions was 98%. Thermodynamic parameters revealed the feasibility and spontaneity nature of the adsorption process and that the adsorption kinetics of pb(II) and Cu(II) ions follow a pseudo-second-order kinetic model.

`

1. Introduction

Heavy metals contamination of industrial wastewater is a significant universal problem and causes a detrimental effect on human health and environment if not managed efficiently. It is thus very important to remove these heavy metals from wastewater before discharging them into the environment.

The removal of heavy metals, such as mercury, lead, thallium, cadmium, arsenic, chromium, nickel and copper from natural waters has attracted considerable attention because of their harmful effects on environment and human health. These metals are dangerous since they do not have the ability to reduce and convert to the less toxic compounds and accumulate in the environment. The toxicity of metals in various conditions is different and is dependent on factors such as concentration, environmental conditions, contact time, and other physical, chemical and biological agents [1].

Heavy metals removal methods include chemical precipitation, membrane filtration, ion exchange, liquid–liquid extraction, adsorption and biosorption [2]. Among these methods, adsorption has increasingly received more attention because it is simple and cost effective [3, 4]. Adsorption of metals by using nanoparticles is a compatible technology for the environment and has been studied as an effective factor for eliminating organic pollutants and heavy metal ions from water and wastewater samples in recent years [5]. The main factors affecting the adsorption are pH, temperature,

* Corresponding author:
E-mail: baseri@du.ac.ir

volatility, particle size (surface area), the structural characteristics of adsorbent, adsorbent amount, initial concentration of metal ions, contact time, sediment time and the presence of competing ions [6,7].

The reasons for widespread use of nanoparticles in adsorption are high surface area, more active places, high absorption efficiency, high reactivity and the ability of nanoparticles to disperse in aqueous solutions. Nano materials usually show more reactivity and higher ability to adsorb than normal materials. Higher surface to mass ratio of nanoparticles greatly increases adsorption capacities of nanoadsorbents. In addition to having a large specific surface, nanoparticles have a unique adsorption property due to the different distribution of reactive surfaces and irregular surface areas. Among these nanoparticles, iron nanoparticles have attracted more attention due to the abundance, cheapness, non-toxic, rapid response and high efficiency for the removal of pollutants from contaminated water [8, 9].

The use of magnetite (Fe_3O_4) nanoparticle as an adsorbent in water treatment provides a suitable and comfortable approach for separating and removing the pollutants by applying external magnetic fields. Bare magnetite nanoparticles are sensitive to air oxidation and are easily aggregated in aqueous systems [10]. Thus, for the application of these nanoparticles in different potential fields, the consolidation of the iron oxide particles by surface modification is desirable.

Several chemical methods that can be used to synthesize magnetic nanoparticles are co-precipitation, reverse micelles and micro-emulsion technology, sonochemical reactions, hydrothermal reactions, sol-gel syntheses, hydrolysis and thermolysis of precursors, flow injection syntheses, and electrospray syntheses [11]. For heavy metal removal applications, a sufficient surface modification of the nanoparticles is an important issue regarding both selectivity and aqueous stability of these materials. To this end, in the last two decades, organic and inorganic functionalized magnetite nanoparticles have been developed and modifications of the abovementioned synthesis methods have been proposed. These functionalized magnetic nanoparticles were found to be chemically stable, cost-effective and environmental friendly in nature compared to bare magnetite nanoparticles.

In the present work, magnetic iron oxide nanoparticles were prepared and functionalized with different kinds of coatings (organic acids including citric acid, ascorbic acid, and salicylic acid, starch as a polysaccharide and saccharose as a kind of disaccharide and a kind of natural zeolite named clinoptilolite from the West Semnan, Iran). Moreover, the efficiency and adsorption characteristics of the produced particles for the removal of toxic metal ions from wastewater were investigated by batch experiments. The batch adsorption performances of nanoadsorbents are determined by operational parameters such as pH, temperature, contact time and adsorbent dosage. In order to study the performance of nanoadsorbents on the adsorption of heavy metals, kinetics (pseudo first and pseudo second order) and thermodynamics studies were utilized.

Because of their higher surface area, the synthesized nano-adsorbents have more sensitivity and selectivity toward heavy metal ions compared to the bare magnetite nanoparticles. Also, these nano-adsorbents could be easily separated from the aqueous solutions by applying an external magnetic field and no centrifugation or filtration is needed. The presented method gives an efficient and cost effective route with very low detection limits and can be applied to the determination of trace amounts of these heavy metal ions in aqueous samples.

2. Materials and methods

2.1. Materials and methods

All of the following chemicals and reagents were of analytical grade and were used without any further purification. Ferric chloride ($FeCl_3 \cdot 6H_2O$), ferrous sulfate ($FeSO_4 \cdot 7H_2O$), ammonia solution, sodium hydroxide (NaOH), sodium chloride (NaCl) and double-distilled deionized water were used for preparing the solutions. We also purchased all of the coatings (citric acid ($C_6H_8O_7$), ascorbic acid ($C_6H_8O_6$), salicylic acid ($C_7H_6O_3$), starch ($(C_6H_{10}O_5)_n$ and saccharose) from the Aldritch Company

(Sigma–Aldrich, Steinem, Germany). Natural zeolite clinoptilolite was obtained from West Semnan, Iran.

We used co-precipitation method for the synthesis of bare magnetite MNPs. In order to prepare Fe_3O_4-acid, Fe_3O_4-starch and Fe_3O_4-saccharose nano-adsorbents, 6.1 g of $FeCl_3.6H_2O$ and 4.2 g of $FeSO_4.7H_2O$ were dissolved in 100 mL of distilled water and heated at 100 °C for 1 h. Then 12 mL of ammonium hydroxide (25%) was added dropwise to the mixture. After 30 minutes, temperature of the system decreased to 80 °C. Then 0.5 g of the desired coatings were dissolved in 50 mL of distilled water and added to the mixture. The mixture was stirred at 80 °C for 1 h and then cooled down to room temperature. The black or dark brown precipitates were collected by centrifugation and washed with deionized water and acetone for several times and dried at 70 °C for 5 h.

The composite of Fe_3O_4 sorbent containing natural zeolite was prepared by the co-precipitation method as follows: First of all, for the activation of zeolite 10 mL of H_2SO_4-HCl (%10) solution was added to the zeolite sample and the mixture was relaxed for 2 h. Then the acid was evacuated and the sample was washed with deionized water 3 times and dried at 150 °C for 2 h. After activation of zeolite, it was added to the Fe_3O_4 sample. Just like the last stage, the mixture was stirred at 80 °C for 1 hour and then cooled down to room temperature. The black precipitate was collected by centrifugation and washed with deionized water and acetone for several times and dried at 70 °C for 5 h.

2.2. Characterizations

The surface functional groups of Fe_3O_4-Cit were determined by Fourier transform infrared spectroscopy (Spectrum RX I). X-ray diffractometer (D8-Advance, Bruker AXS, Cu K α1, λ=1.54 °A) was used for the determination of phase composition of the nano-adsorbents. Scanning electron microscopy (JEOL, JSM 6490 LV) observations of the prepared nanoparticles were carried out at an electron acceleration voltage of 15 kV. Thermogravimetric analysis was performed on a thermal analysis system (Model: STA 503). For TGA measurements, the weight losses of the dried samples were monitored under N_2 from room temperature to 600 °C at a rate of 6 °C/min.

2.3. Heavy metals adsorption tests

Pb(II) and Cu(II) are considered as toxic pollutants in water resources and their efficient removal from wastewater is important. Therefore, adsorption of heavy metal ions is reported in many papers [29-36]. In Table (1) some of these papers are reviewed. To estimate the adsorption ability of our samples, heavy metal adsorption tests were carried out. Hydrated $Pb(NO_3)_2$ and $Cu(NO_3)_2$ were used as the sources of mentioned heavy metal ions, respectively. The pH values of the solutions were adjusted using NaOH or HCl. In a typical removal procedure, citric acid coated Fe_3O_4 nanoparticles were added into 25 mL of Pb(II). solution (10 mg/L), sealed and shaken for 4 h with 500 rpm at room temperature. After shaking, the mixtures were placed under an external magnetic field and the magnetite sample was separated from the solution. Heavy metals concentration in the supernatant solution was measured by using both gravimetric method and atomic adsorption spectroscopy (Chemtech analytical CTA-2000). The samples were analyzed in triplicates and the average values were used in the graphs. The adsorption capacity and percentage removal were roughly estimated by using Eqs. (1) and (2), respectively [12, 13].

$$q_e = \frac{(C_0 - C_e)}{W} \times V \quad (1)$$

$$\text{Removal efficiency (\%)} = \frac{(C_0 - C_e)}{C_0} \times 100 \quad (2)$$

Where q_e (mg/g) is the adsorption capacity at equilibrium, C_0 is the initial concentration of adsorbate (mg/L); C_e is concentration of adsorbate at equilibrium in (mg/L); V is volume of solution in (L) and W is mass of adsorbent (g).

3. Results and discussions

3.1. Characterization of adsorbents

In order to study the structure of clinoptilolite, the sample was analyzed with FTIR spectroscopy in the spectral regions 400 to 4000 cm^{-1}. Figure 1a-b shows the FTIR spectra of non treated clinoptilolite and acid-treated clinoptilolite, respectively. In the FTIR spectrum of clinoptilolite, the symmetric stretch bands at 750 and 490 cm^{-1} and asymmetric stretch band at 1250 are related to the vibration of Al – O or Si – O bond [14]. Also, Figure 2

presents the FTIR spectra of bare magnetic nanoparticles, starch coated magnetic nanoparticles, citric acid coated magnetic nanoparticles, and zeolite coated magnetic nanoparticles. The low intensity absorption band at 570 cm^{-1} was observed for all three types of magnetite samples tested, and it can be associated with the Fe-O stretching vibration for the magnetite nanoparticles. Since starch mainly consists of amylose and amylopectin, three peaks appeared at 1020, 1080 and 1150 cm^{-1} for magnetite-starch nanoparticles. The peaks at 1080 and 1150 cm^{-1} are associated with the C-O stretching vibrations in the C-O-H groups, while the 1150 cm^{-1} peak corresponds to the C-O stretching vibration in the C-O-C groups, which is in agreement with the report by Huang et al. [15]. The two peaks at 1630 and 3400 cm^{-1} are related to the bare magnetite and magnetite-starch samples, respectively. Unlike the bare magnetite sample, highly intensified peaks were observed for the starch coating magnetite sample due to the H-bonded OH groups of amylose and amylopectin of starch, which is in complete agreement with Huang et al. and Maity et al. [15, 16]. Also, there is a large and intense band at around 3450 cm^{-1} in citric acid coated magnetite sample that could be assigned to the structural OH groups, traces of molecular water, or citric acid. The 1700 cm^{-1} peak determinable to the C-O vibration from the COOH group of citric acid shifts to an intense band at around 1600 cm^{-1} for the magnetite coated with citric acid, revealing the binding of a citric acid radical to the Fe_3O_4 surface as shown in Figure 2c. The spectrum of magnetic-clinoptilolite did not primarily differ from the zeolite in the range of 400 to 4000cm^{-1}. In comparison with Fe_3O_4, FTIR spectrum of magnetic-clinoptilolite in the range of 440-580cm^{-1} shows vibration bands that are related to Fe-O functional groups. This fact indicates that Fe_3O_4 structure did not change in this process.

Table 1. Comparison between the reported results of some papers for the removal of heavy metals from water resources

	Researcher name(s)	Ion(s) removed	Absorbent	Studied parameters	Reference
1	**N. N. Nassar**	Pb(II)	Fe_3O_4	**1**. Contact time, **2.** Initial concentration of Pb (II), **3**. pH, **4**. Coexisting cations, **5**. Temperature	[29]
2	**Z. K. Sarkar,** **F. K. Sarkar**	Pb(II)	Fe_3O_4	**1.** pH, **2**. Type of eluent, **3**. contact time	[30]
3	**T. Poursaberi,** **H. Ghanbarnejad,** **V. Akbar**	Pb(II)	Fe_3O_4/porphyrin	**1.** pH, **2**. Contact time, **3**. Sorbent dosage, **4**. Co-existing cations	[31]
4	**J. F. Liu, Z. S. Zhao,** **G. B. Jiang**	Hg(II), Pb(II), Cd(II), Cu(II)	Fe_3O_4/Humic acid	**1**. pH, **2.** Real Water Matrix	[32]
5	**C. M. Chou,** **H. L. Lien**	Zn(II)	Fe_3O_4/dendrimer	**1**. pH	[33]
6	**M. A. Karimi,** **M. Kafi**	Ni(II)	Fe_3O_4/alumina /dimethylglyoxim /sodium dodecyl sulfate	**1**. pH, **2**. Magnetic separation time, **3**. sample volume, 4. nanoparticles' amount	[34]
7	**A. Z. M. Badruddoza,** **A. S. H. Tay, P. Y. Tan,** **K. Hidajat, M. S. Uddin**	Cu(II)	Fe_3O_4/ Carboxymethyl-β-cyclodextrin	**1.** initial pH, **2**. Temperature, **3.** Contact time	[35]
8	**S. H. Huang,** **D. H. Chen**	Cu(II) Cr(VI)	Fe_3O_4/diethylenetriamine	**1.** Initial pH	[36]

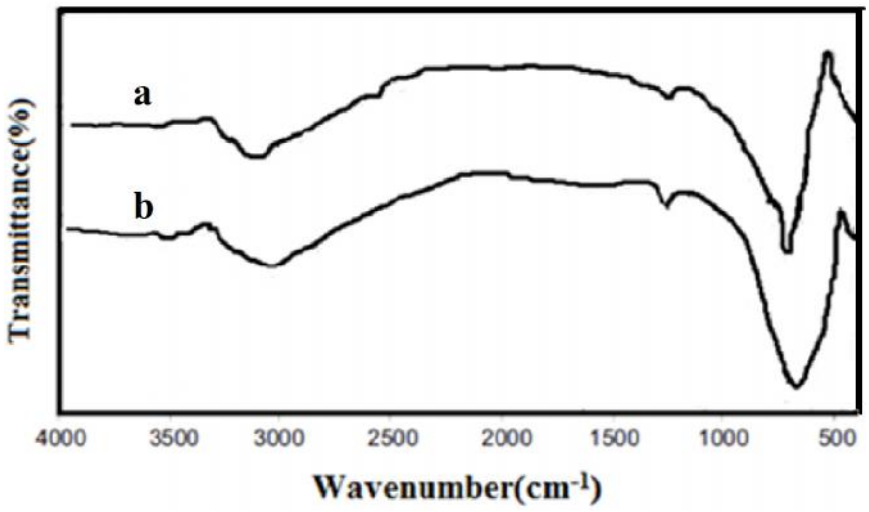

Fig. 1. FTIR spectra of (a) non treated clinoptilolite and (b) acid-treated clinoptilolite

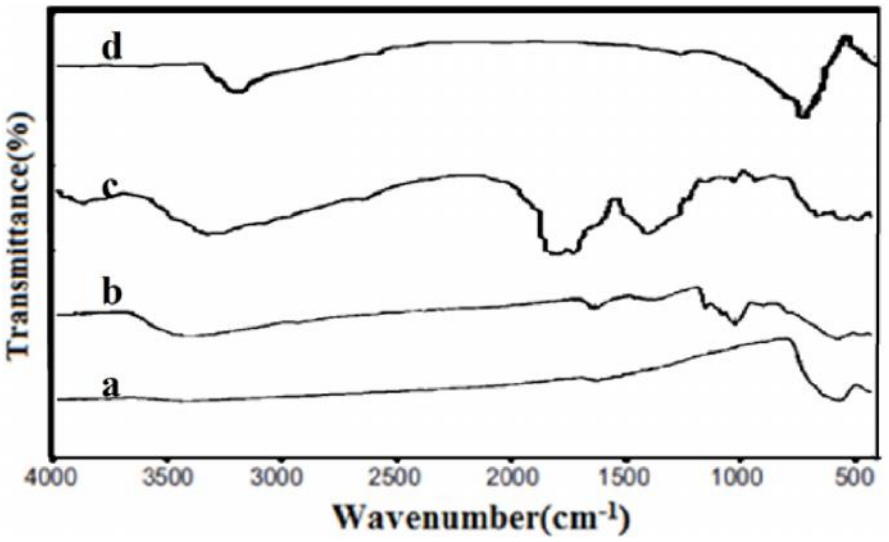

Fig. 2. FTIR spectra of magnetic nanoparticles: (a) bare magnetic nanoparticles, (b) starch coated magnetic nanoparticles, (c) citric acid coated magnetic nanoparticles, (d) clinoptilolite zeolite coated magnetic nanoparticles

The crystalline structures of the nanoparticles were identified with XRD (Figures 3 and 4). For Fe_3O_4, diffraction peaks with 2θ at 30.2°, 35.5°, 43.3°, 57.2°, and 62.8° were observed, indicative of a cubic spinel structure of the magnetite [17]. The same set of characteristic peaks were also observed for Fe_3O_4-citric acid and Fe_3O_4-starch, indicating the stability of the crystalline phase of magnetite nanoparticles during coating surface functionalization and were in common with previous reports [18, 19]. As shown in figure 4, the Fe_3O_4-clinoptilolite pattern shows three crystalline peaks with 2θ° at 35°, 59° and 62° related to the 311, 511 and 440 crystallographic planes of the face-centered cubic (FCC) iron oxide nano crystals [20]. The average particle sizes of the magnetite nanoparticles were in the ranges of about 15–35 nm and were calculated by using the Scherrer's equation as follows:

$$D_c = \frac{0.9\lambda}{L.C\ \theta} \quad (3)$$

The overall appearance and outer surface of ascorbic acid coated magnetite were studied by FE-SEM images of the prepared samples and are shown in Figures 5a-b. A spot size was about 75 nm for coated sample.

TGA curve of the bare MNPs shows a weight loss of about 2% below 150 °C which can be attributed to the loss of adsorbed water in the sample. After that, an unexpected weight gain takes place within the temperature range of 150 to 200 °C. This weight gain might be due to the oxidation of magnetite to maghemite [21]. The total weight loss for this sample at this temperature range is about 3%. For Fe_3O_4-starch, the weight loss at temperatures below 220 °C can be attributed to water desorption and a drastic weight loss of about 7% from 220 to 600 °C is due to the loss or decomposition of starch coating from the sample. Also, the TGA curve for Fe_3O_4-citric acid exhibits two steps of weight loss. The first weight loss can be attributed to the loss of residual water in the sample and the second one is due to the loss of citric acid in the range of 200–600 °C. The total weight loss for this sample is about 13%. So, the TGA curves of these three samples confirm the successful modifications of Fe_3O_4 nanoparticles

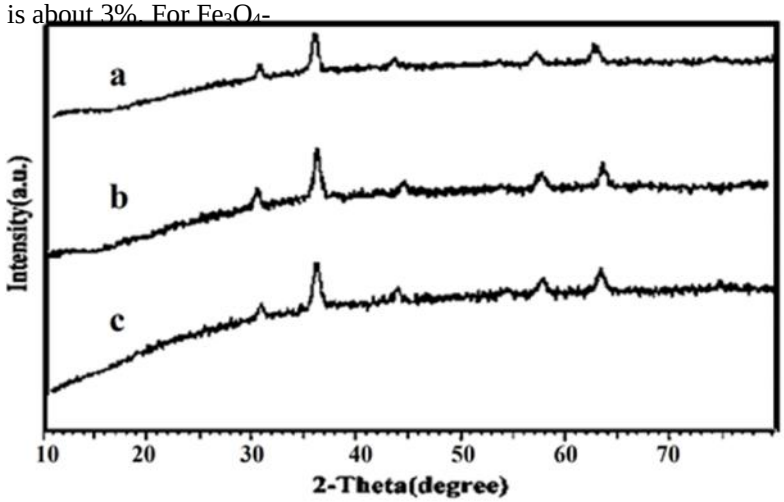

Fig. 3. XRD pattern of magnetic nanoparticles: (a) bare magnetic nanoparticles, (b) citric acid coated magnetic nanoparticles, (c) starch coated magnetic nanoparticles

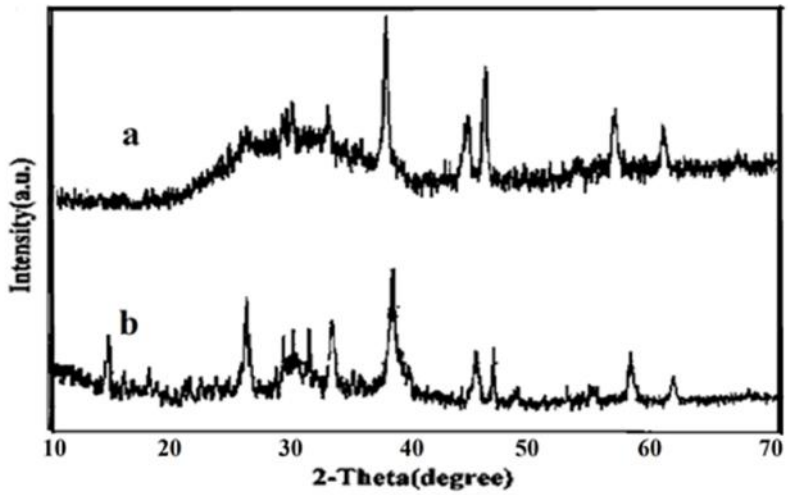

Fig. 4. XRD pattern of magnetic nanoparticles: (a) bare magnetic nanoparticles, (b)clinoptilolite coated magnetic nanoparticles

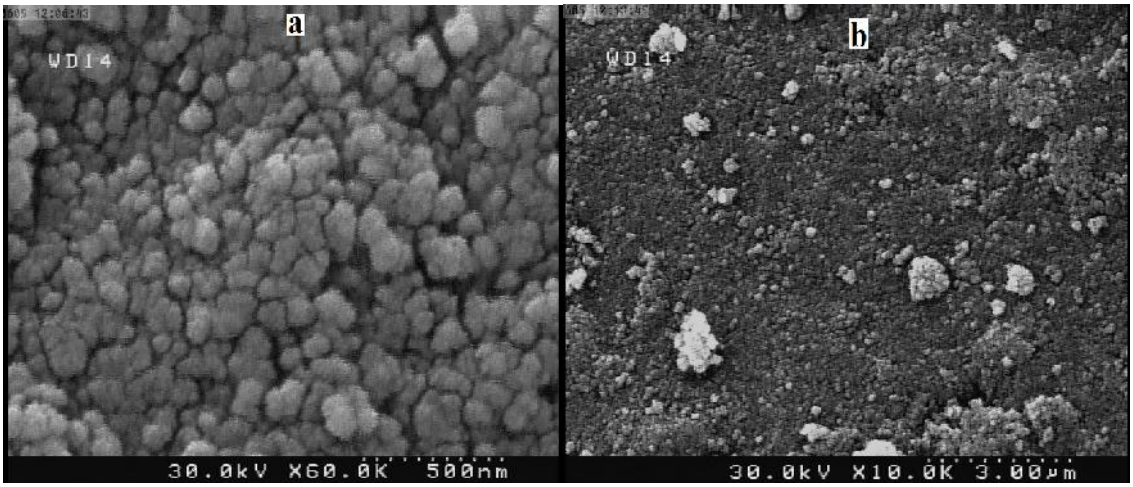

Fig. 5. SEM images of ascorbic acid coated magnetic nanoparticles.

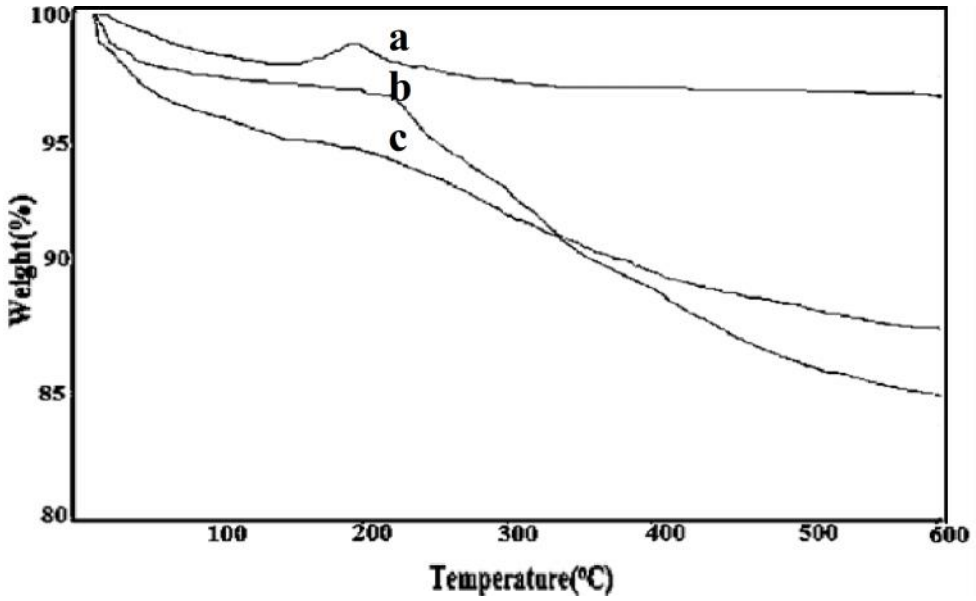

Fig. 6. TGA curves for magnetic nanoparticles: (a) bare magnetic nanoparticles, (b) starch coated magnetic nanoparticles, (c) citric acid coated magnetic nanoparticles

3.2. Heavy metals adsorption

3.2.1. Effect of pH

In adsorption processes pH studies are very important to determine the charge on the surfaces of adsorbents by their functional groups and also determine the speciation of metals in solutions [23]. Figure 7 shows pH dependent removal of pb(II) toxic metal ion by different forms of nanoadsorbents. The pH study of heavy metal ions adsorption on the surface of Fe_3O_4 nanoadsorbents was observed in the range of 2-12. It has been observed that the removal efficiency percentage of pb(II) and Cu(II) metal ions is strongly dependent on the pH of the solution and with an increase in the initial pH of the solution from 2 to 10 the adsorption capacity and removal efficiency strongly increased. On the other hand, the removal efficiency percentage was found to be constant or even decreased at the pH values higher than 10, as

shown in Figure 7 and Table 2. By using citric acid and natural zeolite as the coating of magnetite nanoparticles, almost 100% removal of pb(II) and Cu(II) ions from wastewater was obtained at higher pH. From the obtained results it seems that pH 10 is the best pH for removal of heavy metals. The suppressed adsorption of metal ions at low pH implies that acid treatment is a possible and useful method to regenerate these nanoadsorbents The effects of temperature on the adsorption under optimized conditions are explained in Figure 8 and Table 3. It was observed that adsorption and removal of pb(II) and Cu(II) increased with increases in temperature from 293 K to 313 K and further decreases at higher temperatures. Probably the observed decreases in the removal of these heavy metals with temperature were due to the weakening of the adsorptive forces between the active sites and the adsorbate species on the adsorbents surfaces.

3.2.2. Effect of temperature

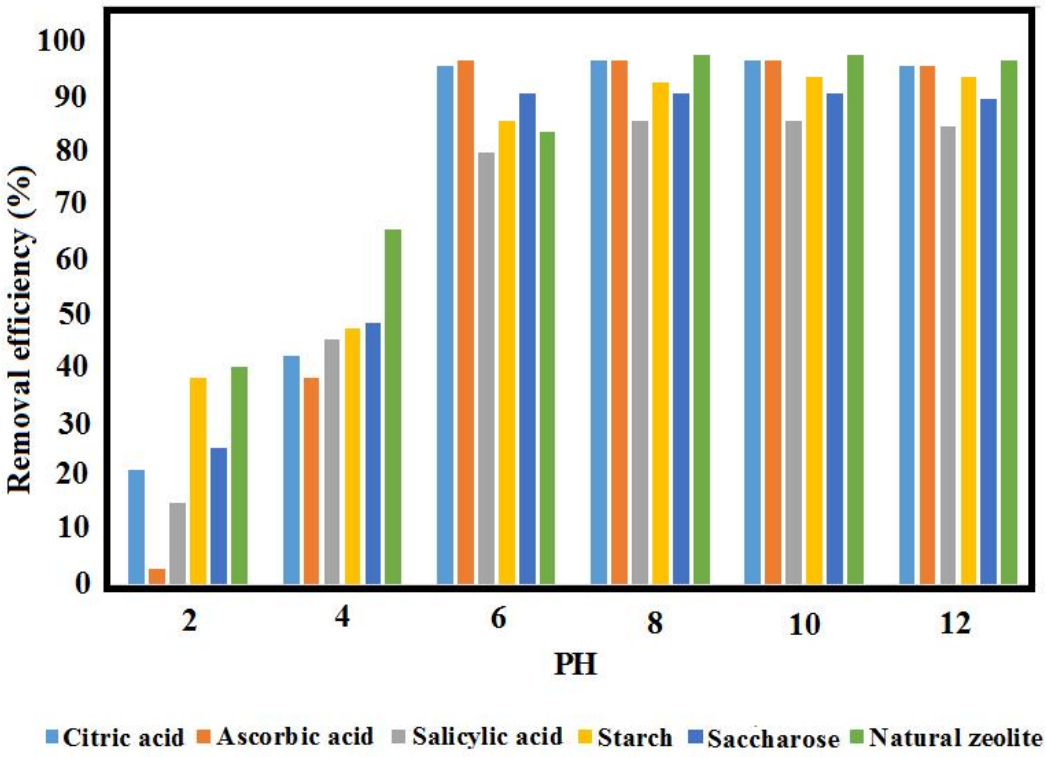

Fig. 7. Effect of pH on the removal of pb(II) (adsorbents dose: 0.2 g, pb(II) concentration: 25 mg/L)

Table 2. Effect of pH on the removal of Cu(II) (adsorbents dose: 0.2 g, Cu(II) concentration: 25 mg/L)

pH	Citric acid	Ascorbic acid	Salicylic acid	Starch	Saccharose	Natural zeolite
2	44%	39%	28%	38%	30%	85%
4	46%	41%	44%	45%	34%	91%
6	64%	50%	65%	68%	53%	95%
8	96%	85%	84%	88%	80%	97%
10	97%	86%	84%	88%	80%	98%
12	97%	86%	84%	87%	79%	98%

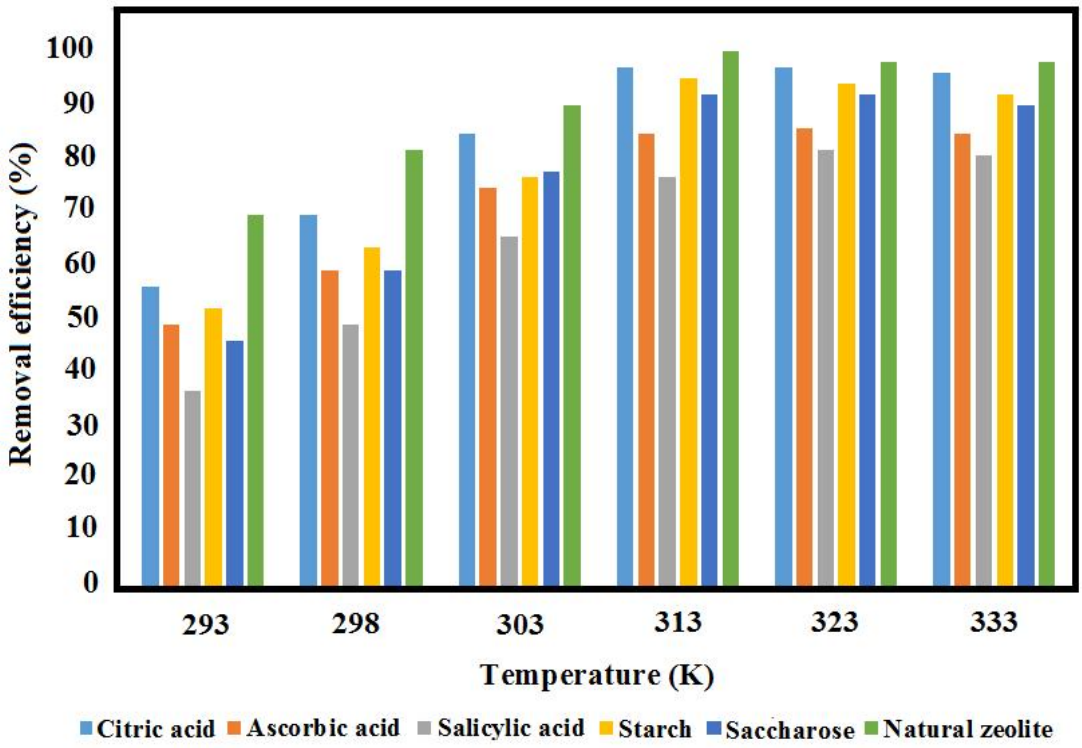

Fig. 8. Effect of temperature on the removal of pb(II) (adsorbents dose: 0.2 g, pb(II) concentration: 25 mg/L)

Table 3. Effect of temperature on the removal of Cu(II) (adsorbents dose: 0.2 g, Cu(II) concentration: 25 mg/L)

Temperature(K)	Citric acid	Ascorbic acid	Salicylic acid	Starch	Saccharose	Natural zeolite
293	50%	48%	33%	61%	45%	64%
298	67%	59%	47%	70%	58%	73%
303	82%	73%	60%	84%	77%	86%
313	94%	81%	74%	92%	90%	95%
323	94%	80%	73%	91%	90%	94%
333	92%	79%	72%	91%	89%	93%

3.2.3. Effect of the contact time

The effect of the contact time on the efficient removal of pb(II) and Cu(II) heavy metal ions was investigated at different time intervals 10, 20, 30, 40, 50, 60 min. The results of using different kinds of nanoadsorbents for the removal of pb(II) ions are shown in Figure 9 and Table 4. The removal efficiency percentage of heavy metal ions increased by increasing the contact time to 50 min. The fast removal of pb(II) ions 98% was observed by using natural zeolite as the coating of the magnetite nanoparticles. Then the curve reached the equilibrium stage and no increase was observed. This is because after this time the adsorptive sites of adsorbents were blocked. According to the results obtained from the experiments, the contact time of 50 min could be selected for further investigation.

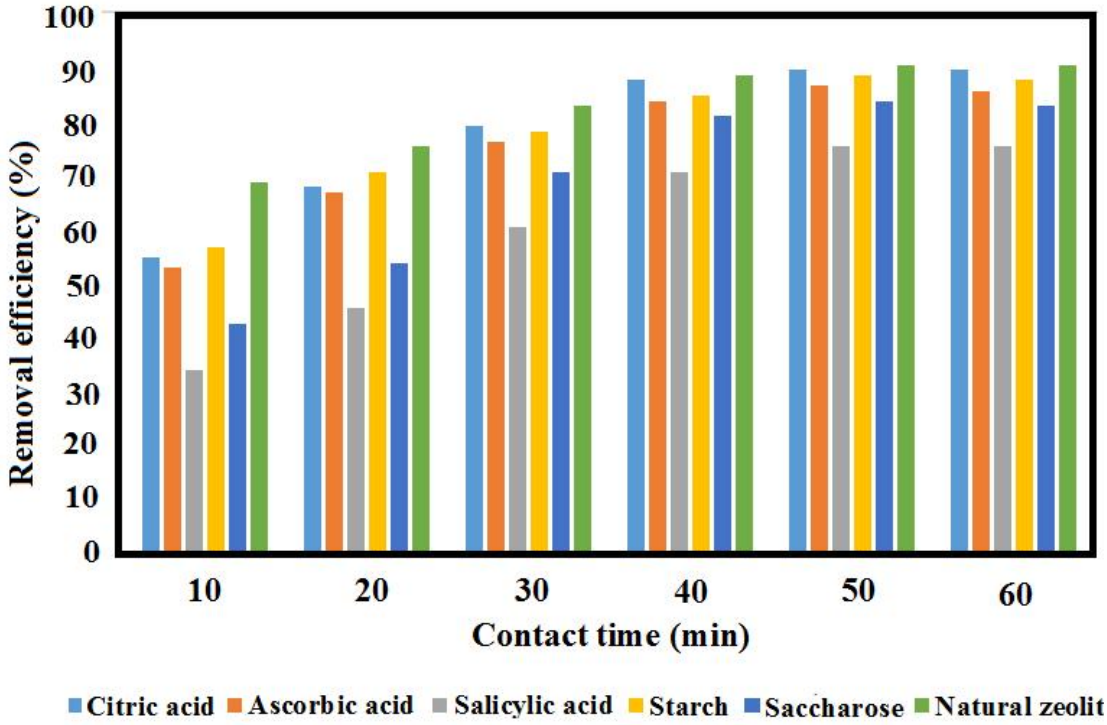

Fig. 9. Effect of contact time on the removal of pb(II) (adsorbents dose: 0.2 g, pb(II) concentration: 25 mg/L)

Table 4. Effect of contact time on the removal of Cu(II) (adsorbents dose: 0.2 g, Cu(II) concentration: 25 mg/L)

Contact time(min)	Citric acid	Ascorbic acid	Salicylic acid	Starch	Saccharose	Natural zeolite
10	59%	50%	41%	50%	38%	64%
20	69%	63%	53%	62%	51%	74%
30	78%	71%	64%	75%	63%	84%
40	90%	82%	73%	87%	74%	92%
50	93%	88%	81%	93%	81%	96%
60	93%	88%	80%	92%	81%	96%

3.2.4. Effect of the adsorbent dose

In order to evaluate the adsorbent dose effect on the efficient removal of heavy metal ions, the adsorption experiments were carried out with different concentrations of surface engineered MNPs. 40, 80, 120, 160, 200 and 240 mg of each magnetic nano-adsorbent was used and the results revealed that the removal efficiency increases with increasing the concentration of nanoadsorbents (Figure 10 and Table 5). Compared to the usual sorbents, magnetic nanoparticles sorbents have higher surface areas and reasonable results are obtained with fewer amounts of MNPs sorbents. Thus, the efficiency of simultaneous adsorption of heavy metal ions can be described on the basis of surface functionality, competitive affinity of heavy and toxic metal ions for Fe_3O_4, the amount of surface charge, and availability of active surface sites on Fe_3O_4 nanoparticles. The maximum amount of heavy metal removal for all of the samples was obtained by 0.2 g use of nanoadsorbents.

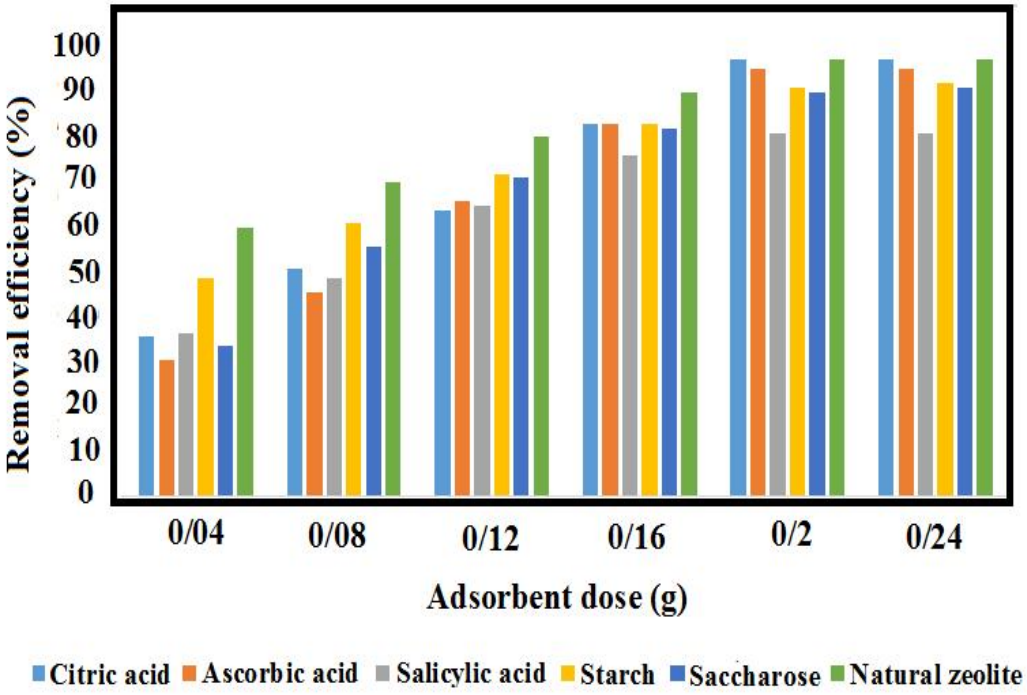

Fig. 10. Effect of adsorbent dose on the removal of pb(II) (pH: 10, pb(II) concentration: 25 mg/L)

Table 5. Effect of adsorbent dose on the removal of Cu(II) (pH: 10, Cu(II) concentration: 25 mg/L)

Adsorbent dose(g)	Citric acid	Ascorbic acid	Salicylic acid	Starch	Saccharose	Natural zeolite
0.04	18%	15%	20%	35%	20%	55%
0.08	34%	39%	42%	55%	42%	69%
0.12	60%	65%	60%	71%	65%	83%
0.16	82%	81%	78%	82%	74%	95%
0.20	96%	86%	85%	88%	79%	98%
0.24	96%	86%	85%	88%	78%	98%

3.2.5. Adsorption thermodynamics

The effect of temperature on the adsorption isotherm was investigated under isothermal conditions in the temperature range of 293–313K and optimal conditions. Thermodynamic parameters such as ΔG^o (KJ/mol), ΔH^o (KJ/mol), and entropy ΔS^o (J/mol.k) are calculated using the following thermodynamic functions [24, 25]:

$$\Delta G^0 = -RT \ln K_d \quad (4)$$

$$\ln K_d = -\frac{\Delta H^0}{R} + \frac{\Delta S^0}{R} \quad (5)$$

$$K_d = \frac{q_e}{C_e} \quad (6)$$

$$\Delta G^0 = \Delta H^0 - T\Delta S^0 \quad (7)$$

where R is the universal gas constant (8.314 J/mol K), T is the absolute temperature in Kelvin, K_d is distribution coefficient, q_e (mg/g) is the equilibrium concentration of metal ions adsorbed onto magnetite based nanoadsorbents and C_e (mg/L) is the remained concentration of metal ions in the solution.

The calculated values for thermodynamic parameters are reported in Table 6. The negative values of ΔH^0 confirm the exothermic nature of adsorption and the positive values of ΔS^0 is caused by the increase in the degree of freedom or randomness at the adsorbent-adsorbate

interface during the adsorption of Ni(II) at different temperatures. Also, the negative values of ΔG^0 indicate the feasibility of the process and spontaneous nature of pb(II) and Cu(II) ions adsorption onto these nanoadsorbents [26].

3.2.6. Adsorption kinetics

The adsorption kinetics of metal ions onto different adsorbents was investigated with the help of the pseudo-first order and pseudo-second order model. The pseudo-first order kinetic model is expressed by the following equation [27]:

$$ln(q_e-q_t) = ln\ q_t - k_1 t \quad (8)$$

Where q_e and q_t refer to the adsorption capacity of metal ions (mg/g) at equilibrium and at any time, t (min), respectively, and k_1 is the rate constant of pseudo-first order adsorption (min^{-1}). The slope of the linear plot of ln (q_e-q_t) versus t is used to determine k_1.

The pseudo-second order kinetic rate equation is expressed as follows [28]:

$$\frac{t}{q_t} = \frac{1}{k_2 q_e^2} + \frac{1}{q_e} t \quad (9)$$

Where k_2 is the rate constant of pseudo-second order adsorption (g/mg min).

The calculated values for kinetic parameters are reported in Table 7. It was found that the correlation coefficients (R^2) for the pseudo-first order kinetic model of mentioned nanoadsorbents are less than the correlation coefficient (R^2) for the pseudo-second order adsorption model. The adsorption data are well represented by pseudo-second order kinetic model and this means that chemical adsorption is the main rate determining step.

3.2.7. Desorption and reusability of nanoadsorbents

As shown in Table 8, to study the desorption of pb(II) and Cu(II) ions loaded magnetite based nanoadsorbents, different concentrations of HNO_3 as desorption media (0.05, 0.1, 0.15 and 0.2 M) were used. The maximum values of desorption efficiency was observed by using 0.20 M HNO_3. To detect the reusability of adsorption–desorption, five times desorption were carried out by using the same adsorbent. The related results for reusability experiments are reported in Table 9. In this study, the initial concentration of pb(II) and Cu(II) ions was 25 mg/L, the adsorbent dose was 0.2 g, the reaction temperature was 298 K, and the pH value was 3. The obtained results showed that nanoadsorbents have good reusability and suitability for the removal of pb(II) and Cu(II) ions. It was observed that with increasing in the

Table 6. Thermodynamic parameters for the adsorption of Cu(II) and pb(II) ions onto different adsorbents

Analyte	Adsorbent	Temperature(k)	ΔG^0(kJ/mol)	ΔH^0(kJ/mol)	ΔS^0(J/mol K)
Copper	Magnetite-clinoptilolite	293 303 313	-2.826 -5.857 -6.673	-577.077	0.192
Lead	Magnetite-citric acid	293 303 313	-2.247 -5.858 -6.045	-581.828	0.190

Table7. Kinetic parameters obtained for the Ni(II) adsorption by different adsorbents (C_i = 25 mg/L, Tem = 303 K)

Analyte	Adsorbent	Pseudo first order			Pseudo second orde		
		k_1 (min^{-1})	qe.cal (mg/g)	R^2	k_2 (min^{-1})	qe.cal (mg/g)	R^2
Copper	Magnetite-clinoptilolite	0.086	13.423	0.971	0.011	13.812	0.998
Lead	Magnetite-citric acid	0.079	10.783	0.989	0.010	14.225	0.998

cycle numbers, the uptake capacity of metal ions on the nanoadsorbents slowly decreased. Effectiveness recovery of metal ions from the solid phase was determined by the following relation:

$$R\ (\%) = \frac{C_d}{C_a} \times 100 \quad (10)$$

4. Conclusion

A simple method was developed for the adsorption and removal of lead and copper heavy metal ions from artificial wastewater sample. In summary, a simple, environmentally friendly, timesaving and low cost co-precipitation method was applied to obtain different kinds of magnetic nanoadsorbents with well defined diameters. These nanoparticles have relatively high adsorption capacity compared to similar materials because of their smaller size. The size of the produced magnetite nanoadsorbents was estimated by both X-ray diffraction analysis and scanning electron microscopy. The adsorption capacity of bare Fe_3O_4 is about 75% for Pb ions and 78% for Cu ions, but by using various coatings, it increased to higher than 90% for similar conditions. The negative values of ΔG^0 confirm the feasibility and spontaneity of the pb(II) and Cu(II) ions adsorption. Desorption and reusability studies showed that the nanoadsorbents can be used repeatedly, without decreasing the adsorption capacity. Therefore, these nanoadsorbents are recommended as fast, effective and cheap adsorbents for rapid removal and recovery of many heavy metal ions from wastewater samples.

Table 8. Reusability percentage of nanoadsorbents

Analyte	Adsorbent	HNO_3 concentration(M)	Reusability percentage
Copper	Magnetite-clinoptilolite	0.05	80
		0.10	93
		0.15	94
		0.20	95
Lead	Magnetite-citric acid	0.05	71
		0.10	90
		0.15	92
		0.20	93

Table 9. Reusability of Fe_3O_4 based nanoadsorbents for adsorption/desorption of metal ions during five cycles

Analyte	Adsorbent	Cycle numbers	Removal percentage
Copper	Magnetite-clinoptilolite	1	96
		2	94
		3	93
		4	92
		5	90
Lead	Magnetite-citric acid	1	96
		2	95
		3	94
		4	92
		5	91

References

[1] N. Sobhi, Removal of heavy metals from industrial wastewater by ash, Ph.D. Thesis, University of Tarbiat Modarres, Tehran, 1998.

[2] I. Zawierucha, C. Kozlowski, G. Malina, "Immobilized materials for removal of toxic metal ions from surface/ground waters and aqueous waste streams", Environ. Sci.: Processes Impacts. J., Vol. 18, 2016, pp. 429-444.

[3] H. Chen, Y. Zhao, A. Wang, "Removal of Cu(II) from aqueous solution by adsorption onto acid-activated palygorskite", Hazard. Mater. J., Vol. 149, 2007, pp. 346–354.

[4] M. Kumari, B.D. Tripathi, "Efficiency of Phragmites australis and Typha latifolia for heavy metal removal from wastewater", Ecotoxicol. Environ. Safe. J., Vol. 112, 2015, pp. 80–86.

[5] Z. Zhang, M. Li, W. Chen, S. Zhu, N. Liu, L. Zhu, "Immobilization of lead and cadmium from aqueous solution and contaminated sediment using nano-hydroxyapatite", Environ. Pollut. J., Vol. 158, 2010, pp. 514-519.

[6] S.M. De Oliveira Brito, H.M.C. Andrade, L.F. Soares, R.P. de Azevedo, "Brazil nut shells as a new biosorbent to remove methylene blue and indigo carmine from aqueous solutions", Hazard. Mater. J., Vol. 174, 2010, pp. 84–92.

[7] M. Dakiky, M. Khamis, A. Manassra, M. Mereb, "Selective adsorption of chromium VI in industrial wastewater using low-cost abundantly available adsorbents", Adv. Environ. Res. J., Vol. 6, 2002, pp. 533–541.

[8] S.R. Kanel, B. Manning, L. Charlet, H. Choi, "Removal of arsenic (III) from groundwater by nanoscale zero– valent iron", Environ. Sci. Technol. Lett., Vol. 39, 2005, pp. 1291-1298.

[9] G. Huang, C. Yang, K. Zhang, J. Shi, "Adsorptive removal of copper ions from aqueous solution using cross-linked magnetic chitosan beads", Chinese. Chem. Eng. J., Vol. 17, 2009, pp. 960-966.

[10] D. Maity, D.C. Agrawal, "Synthesis of iron oxide nanoparticles under oxidizing environment and their stabilization in aqueous and non-aqueous media", Magn. Magn. Mater. J., Vol. 308, 2007, pp. 46-55.

[11] S. Laurent, D. Forge, M. Port, A. Roch, C. Robic, L. Vander Elst, R.N. Muller, "Magnetic iron oxide nanoparticles: Synthesis, stabilization, vectorization, physico-chemical characterizations and biological applications", Chem. Rew. J., Vol. 108, 2008, pp. 2064-2110.

[12] H.R. Tashauoei, H. Movahedian, H. Attar, M.M. Amin, M. Kamali, M. Nikaeen, V.M. Dastjerdi, "Removal of cadmium and humic acid from aqueous solutions using surface modified nanozeolite", Environ. Sci. Technol. J., Vol. 7, 2010, pp. 497–508.

[13] M. Ahmaruzzaman, S.L. Gayatri, "Activated tea waste as a potential low-cost adsorbent for the removal of p-nitrophenol from wastewater", Chem. Eng. Data J., Vol. 55, 2010, pp. 4614–4623.

[14] V. P. Deshpande, B. Prin, "Dielectric study of zeolite clinoptilolite", Eng. Res. Te. J., vol. 1, 2012, p. 2278.

[15] M. Huang, H. Wang, J. Yu, "Studies of biodegradable thermoplastic amylose/kaolin composites: fabrication, characterization, and properties", Polym. Composite J., 2006, pp. 309-314.

[16] D. Maity, D.C. Agrawel, "Synthesis of iron oxide nanoparticles under oxidizing environment and their stabilization in aqueous and non-aqueous media", Magn. Magn. Mater. J., Vol. 308, 2007, pp. 46-55.

[17] T.Z. Yang, C.M. Shen, H.J. Gao, "Highly ordered self-assembly with large area of Fe_3O_4 nanoparticles and the magnetic properties" Phys. Chem. J., Vol. 109, 2005, pp. 23233-23236.

[18] D. Singh, R.K. Gautam, R. Kumar, B.K. Shukla, V. Shankar, V. Krishna, "Citric acid coated magnetic nanoparticles: Synthesis, characterization and application in removal of Cd(II) ions from aqueous solution", Water. Process. Eng. J., Vol. 4, 2014, pp. 233-241

[19] D.H Kim, K.N Kim, K.M Kim, Y.K Lee, "Targeting to carcinoma cells with chitosan- and starch-coated magnetic nanoparticles for magnetic hyperthermia", Biomed. Mater. Res. J., Vol. 88 A, 2009, pp. 1-11.

[20] S. Hosseini, H. Jahangirian, M. H. Shahismail, M. J. Haron, R. Moghaddam, K. Shameli, K. Kalantari, R. Khandanlou, E. Gharibshahi, S. Soltaninejad, "Synthesis and characterization of zeoliteFe_3O_4 nanocomposite by green quick precipitation method," Nanomater. Bios. J., Vol. 8, 2013, pp. 1405-1413.

[21] D. Caruntu, G. Caruntu, Y. Chen, C. O'Connor, G. Goloverda, V. Kolesnichenko, "Synthesis of variable-sized nanocrystals of Fe_3O_4 with high surface reactivity", Chem. Mater. J., Vol. 16, 2004, pp. 5527.

[22] D. Pathania, S. Sharma, "Effect of surfactants and electrolyte on removal and recovery of basic dye by using Ficuscarica cellulosic fibers as biosorbent", J. Ten-side Surfactant Deterg., Vol. 49, 2012, pp. 306–314.

[23] M. Ahmaruzzaman, V. K. Gupta, "Rice husk and its ash as low-cost adsorbents in water and wastewater treatment", Ind. Eng. Chem. Res. J., Vol. 50, 2011, pp. 13589–13613.

[24] A. Eser, T. V. Nüket, T. Aydemir, S. Becerik, A. Dinçer, "Removal of nickel (II) ions by histidine modified chitosan beads", Chem. Eng. J., Vol. 210, 2012, pp. 590-596.

[25] Y. Liu, M. Chen, H. Yongmei, "Study on the adsorption of Cu(II) by EDTA functionalized Fe_3O_4 magnetic nanoparticles", Chem. Eng. J., Vol. 218, 2013, pp. 46-54.

[26] R. Jain, V. K. Gupta, S. Sikarwar, "Adsorption and desorption studies on hazardous dye Naphtha Yellow", J. Hazard. Mater. Vol. 182, 2010, pp. 749–756.

[27] Y. S. Ho, G. McKay, "A comparison of chemisorption kinetic models applied to pollutant removal on various sorbents", Proc. Saf. Environ. Protect., Vol. 76, 1998, pp.332–340.

[28] Y. S. Ho, G. McKay, "Pseudo-second order model for sorption processes". Process. Biochem., Vol. 34, 1999, pp. 451–465.

[29] N. N. Nassar, "Rapid removal and recovery of Pb(II) from wastewater by magnetic nanoadsorbents", J. Hazard. Mater., Vol. 184, 2010, pp. 538–546.

[30] Z. K. Sarkar, F. K. Sarkar, "Selective Removal of Lead (II) Ion from Wastewater Using Superparamagnetic Monodispersed Iron Oxide (Fe_3O_4) Nanoparticles as a Effective Adsorbent", Int. J. Nanosci. Nanotechnol., Vol. 9, 2013, pp. 109-114.

[31] T. Poursaberi, H. Ghanbarnejad, V. Akbar, "Selective Magnetic Removal of Pb(II) from Aqueous Solution by Porphyrin Linked-Magnetic Nanoparticles", J.N.S., Vol. 2, 2013, pp. 417- 426.

[32] J. F. Liu, Z. S. Zhao, G. B. Jiang, "Coating Fe_3O_4 Magnetic Nanoparticles with Humic Acid for High Efficient Removal of Heavy Metals in Water", Environ. Sci. Technol., Vol. 42, 2008, pp. 6949–6954.

[33] C. M. Chou, H. L. Lien, "Dendrimer-conjugated magnetic nanoparticles for removal of zinc (II) from aqueous solutions", J. Nanopart. Res., Vol. 13, 2011, pp. 2099–2107.

[34] M. A. Karimi, M. Kafi, "Removal, preconcentration and determination of Ni(II) from different environmental samples using modified magnetite nanoparticles prior to flame atomic absorption spectrometry", Arabian J. Chem., Vol. 8, 2015, pp. 812–820.

[35] A. Z. M. Badruddoza, A. S. H. Tay, P. Y. Tan, K. Hidajat, M. S. Uddin, "Carboxymethyl-β-cyclodextrin conjugated magnetic nanoparticles as nano-adsorbents for removal of copper ions: Synthesis and adsorption studies", J. Hazard. Mater., Vol. 185, 2011, pp. 1177–1186.

[36] S.H. Huang, D. H. Chen, "Rapid removal of heavy metal cations and anions from aqueous solutions by an amino-functionalized magnetic nano-adsorbent" J. Hazard. Mater., Vol. 163, 2009, pp. 174–179.